Available online at www.sciencedirect.com
ScienceDirect
Journal of the European Ceramic Society 29 (2009) 3063–3068
www.elsevier.com/locate/jeurceramsoc

Effects of Re_2O_3 (Re = La, Nd, Y and Yb) addition in hot-pressed ZrB_2–SiC ceramics

Wei-Ming Guo [a], Jef Vleugels [b,*], Guo-Jun Zhang [a,*], Pei-Ling Wang [a], Omer Van der Biest [b]

[a] *State Key Lab of High Performance Ceramics and Superfine Microstructure, Shanghai Institute of Ceramics, Chinese Academy of Sciences, 1295 Dingxi Road, 200050 Shanghai, PR China*

[b] *Department of Metallurgy and Materials Engineering, Katholieke Universiteit Leuven, Kasteelpark Arenberg 44, B-3001 Leuven, Belgium*

Received 22 December 2008; received in revised form 7 April 2009; accepted 16 April 2009
Available online 14 May 2009

Abstract

ZrB_2–20 vol% SiC composites with 3 vol% Re_2O_3 rare-earth oxide (Re = La, Nd, Y or Yb) were hot pressed to near full-density at 1900 °C. The La_2O_3 and Nd_2O_3 additions not only caused the formation of an amorphous grain boundary phase and enhanced densification, but also resulted in substantial ZrB_2 and SiC grain growth. In contrast, the Y_2O_3 and Yb_2O_3 additions resulted in the formation of crystalline $(Y/Yb)_2Zr_2O_7$ and enhanced densification without ZrB_2 and SiC grain growth. The hardness was improved by the rare-earth oxide addition, especially with Y_2O_3 and Yb_2O_3. The La_2O_3 and Nd_2O_3 only had a minor effect on the fracture toughness, whereas the Y_2O_3 and Yb_2O_3 additions increased the fracture toughness. The type of Re_2O_3 addition was found to influence the nature of the grain boundary and the concomitant fracture and toughening mechanisms.
© 2009 Elsevier Ltd. All rights reserved.

Keywords: Microstructure; Mechanical properties; ZrB_2–SiC; Rare-earth oxides

1. Introduction

Among the ultra-high-temperature ceramics (UHTCs), ZrB_2 is attractive for high-temperature structural applications due to its low theoretical density (6.09 g/cm^3), high melting temperature, high strength, and high thermal and electrical conductivity.[1] SiC is typically added to monolithic ZrB_2 ceramics to improve the strength, fracture toughness and oxidation resistance.[2–6]

Because of the strong covalent bonding and low bulk self-diffusion coefficients of ZrB_2, ZrB_2–SiC ceramics have typically been densified by hot pressing at relatively high temperature. Several studies have concluded that the addition of non-oxides, such as WC, Si_3N_4 or ZrN, enhanced the sinterability and densification of hot-pressed ZrB_2–SiC ceramics.[2,7–9] The addition of oxides as sintering aids, however, has hardly been addressed. Recently, the addition of Y_2O_3 was reported to improve both densification and flexural strength of ZrB_2–SiC ceramics.[10] Because of the similarity in chemical and physical properties, other rare-earth oxides might be as effective as Y_2O_3 in densifying ZrB_2–SiC ceramics. On the other hand, the difference in cationic field strength (z/r^2: valence (z), bond length of Re–O (r)) might result in composites with different properties. For SiC ceramics, Zhou et al. revealed that a decrease in the cationic radius of the Re_2O_3 was accompanied by an increase in Young's modulus, hardness and flexural strength and a decrease in fracture toughness.[11] Usually, Re_2O_3 additions react with the surface SiO_2 on SiC to form an amorphous grain boundary phase. The smaller Re^{3+} ions with bigger field strength make the glass network more compact and tight, producing a stronger intergranular phase, resulting in a higher flexural strength of the SiC ceramics.[11] Moreover, the addition of Re_2O_3 with a smaller Re^{3+} was also reported to result in smaller SiC grain sizes.[12]

In this work, four single rare-earth oxides, i.e. La_2O_3, Nd_2O_3, Y_2O_3 and Yb_2O_3, were chosen as additives for ZrB_2 ceramics containing 20 vol% SiC. The La_2O_3 and Nd_2O_3 belong to the lighter rare-earth oxides and have larger cation radii, whereas the cation radii are smaller for heavier rare-earth oxides such as

* Corresponding authors. Tel.: +32 16 321244; fax: +32 16 321992.
E-mail addresses: jozef.vleugels@mtm.kuleuven.be (J. Vleugels), gjzhang@mail.sic.ac.cn (G.-J. Zhang).

0955-2219/$ – see front matter © 2009 Elsevier Ltd. All rights reserved.
doi:10.1016/j.jeurceramsoc.2009.04.021

Table 1
Starting composition, hot pressing temperature, relative density, and mechanical properties of the ZrB_2–SiC ceramics.

Grade	Starting composition (vol%)	Hot pressing temperature (°C)	Relative density (%)	Vickers hardness (GPa)	Fracture toughness (MPa $m^{1/2}$)
ZS-1900	$80ZrB_2 + 20SiC$	1900	97.5	18.05 ± 0.17	3.6 ± 0.1
ZS-1950	$80ZrB_2 + 20SiC$	1950	99.3	16.89 ± 0.74	4.0 ± 0.4
ZSLa3	$77ZrB_2 + 20SiC + 3\ La_2O_3$	1900	>99.9	19.40 ± 0.16	3.4 ± 0.2
ZSNd3	$77ZrB_2 + 20SiC + 3Nd_2O_3$	1900	>99.9	19.17 ± 0.26	3.7 ± 0.1
ZSY3	$77ZrB_2 + 20SiC + 3Y_2O_3$	1900	99.1	19.86 ± 0.43	4.7 ± 0.1
ZSYb3	$77ZrB_2 + 20SiC + 3Yb_2O_3$	1900	99.7	20.17 ± 0.28	4.9 ± 0.2

Y_2O_3 and Yb_2O_3. The main goal is to examine the effectiveness of the different types of rare-earth oxides as densification aids as well as their influence on the microstructure and mechanical properties of ZrB_2–SiC ceramics.

2. Experimental procedure

The raw materials used were ZrB_2 ($D_{50} = 14\ \mu m$, Gongyi Sanxing Ceramics Materials Co. Ltd., Gongyi, China), SiC ($D_{50} = 0.45\ \mu m$, 98.5%, Changle Xinyuan Carborundum Micropowder Co. Ltd., Changle, China), La_2O_3 (99.95%, SCRC, Shanghai, China), Nd_2O_3 (99.95%, SCRC, Shanghai, China), Y_2O_3 (99.95%, SCRC, Shanghai, China) and Yb_2O_3 (99.9%, ChemPur, Germany). The ZrB_2–SiC composites with and without Re_2O_3 additions are listed in Table 1. The starting powder mixtures were ball milled for 8 h in acetone using Si_3N_4 balls in a planetary ball mill (QM-ISP04, Nanjing University Instrument Plant, China) in nylon containers with a ball to powder mass ratio of 2:1, and dried by rotary evaporation. The powder compacts were hot pressed (ZT-60-22Y, Shanghai Chen Hua Electric Furnace Co. Ltd., China) in a graphite punch/die set-up at 1900 °C for 60 min under a pressure of 30 MPa in argon. The heating rate was 10 °C/min and the load was applied when the temperature reached 1900 °C. In an additional experiment, a ZrB_2–SiC composite without Re_2O_3 addition was hot pressed at 1950 °C for 1 h at 30 MPa (designated ZS-1950).

The final bulk density was measured using the Archimedes method. Relative densities were calculated by dividing measured bulk densities by true densities estimated according to the rule of mixtures. The phase composition was determined by X-ray diffraction (XRD, D/max 2550 V, Tokyo, Japan) on polished cross-sections. The microstructure was investigated by scanning electron microscopy (SEM, XL30-FEG, FEI, Eindhoven, The Netherlands) using secondary electrons. Electron probe microanalysis (JEOL JXA-8100F, Japan) was used to characterize the constituent phases by means of energy-dispersive X-ray spectroscopy (EDS, Oxford INCA energy). For the secondary electron micrographs, the polished cross-sections were acid etched in a solution of water, nitric acid, and hydrofluoric acid (60:20:20, v/v/v). The hardness and fracture toughness were measured by the Vickers indentation method (Model FV-700, Future-Tech Corp., Tokyo, Japan) using a load of 98 N for 10 s on a polished surface. The indentation fracture toughness was calculated according to the equation of Evans and Charles.[13,14]

3. Results and discussion

3.1. Densification, constituent phases and microstructure

The relative densities of the sintered ceramics are summarized in Table 1. The relative density of the undoped ZrB_2–SiC ceramic, hot pressed at 1900 °C and 1950 °C, were 97.5% and 99.3%, respectively. The addition of 5 vol% Re_2O_3 (Re = La, Nd, Y and Yb) increased density to above 99% after hot pressing at 1900 °C. The increased density was accompanied by a change in phase composition and microstructure.

The XRD patterns of milled ZrB_2 powder and the cross-sectioned hot pressed composites are shown in Fig. 1. In all hot-pressed samples, the XRD patterns showed the presence of ZrB_2 as the major phase and SiC as a secondary phase. Monoclinic ZrO_2 was observed in milled powders. Trace amounts of monoclinic ZrO_2 were detected due to oxygen contamination on the surface of ZrB_2 starting powder and additional oxidation during ball milling. In addition, powders were manipulated in air before hot pressing, which may have resulted in oxygen adsorption that could also form surface oxides during heating. This also explained the small amount of ZrO_2 present in the ZS-1900 composite. At a higher sintering temperature of 1950 °C, the ZrO_2 reacted with carbon, presumably from the graphite die/punch

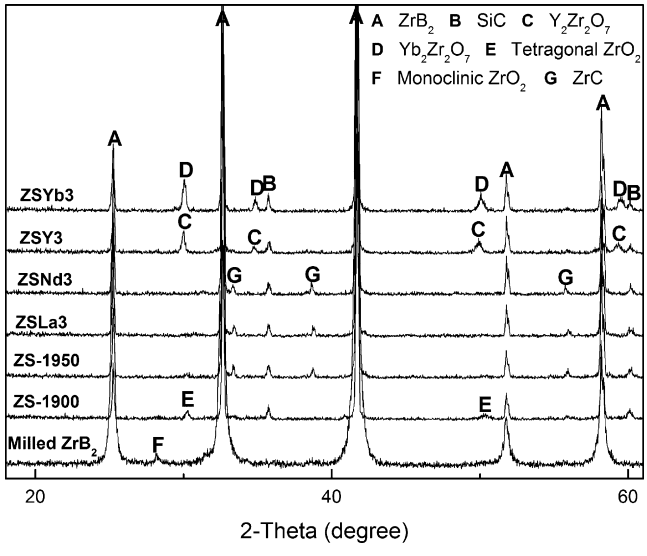

Fig. 1. XRD patterns of milled powders along with ZS-1900, ZS-1950, ZSLa3, ZSNd3, ZSY3, and ZSYb3.

set-up in the hot press to form ZrC, possibly by reaction (1):

$$ZrO_2 + 3C \rightarrow ZrC + 2CO \quad (1)$$

So within the limits of detection of XRD, the ZrO_2 converted to ZrC in ZS-1950. It was interesting to note that the ZSLa3 and ZSNd3 ceramics, hot pressed at 1900 °C, showed similar XRD results as the ZS-1950 grade. This indicates that the La_2O_3 and Nd_2O_3 additions might enhance the carbon diffusion from the graphite die/punch system throughout the densifying powder compact and enhance the ZrO_2 to ZrC conversion, promoting reaction (1) at even lower temperature (1900 °C). Within the resolution limits of XRD, no crystalline La(Nd)-containing phases were detected in ZSLa3 and ZSNd3.

In the ZSY3 and ZSYb3 composites, the addition of Re_2O_3 (Re = Y and Yb) resulted in the formation of $Re_2Zr_2O_7$ instead of ZrO_2 according to the following reaction:

$$2ZrO_2 + Re_2O_3 \rightarrow Re_2Zr_2O_7 \quad (2)$$

Literature reports claim that $Yb_2Zr_2O_7$ can be synthesized from Yb_2O_3 and ZrO_2 powders at 1600 °C.[15]

Backscattered electron images and EDS point analysis results on the constituent phases of ZSLa3 and ZSYb3 are presented in

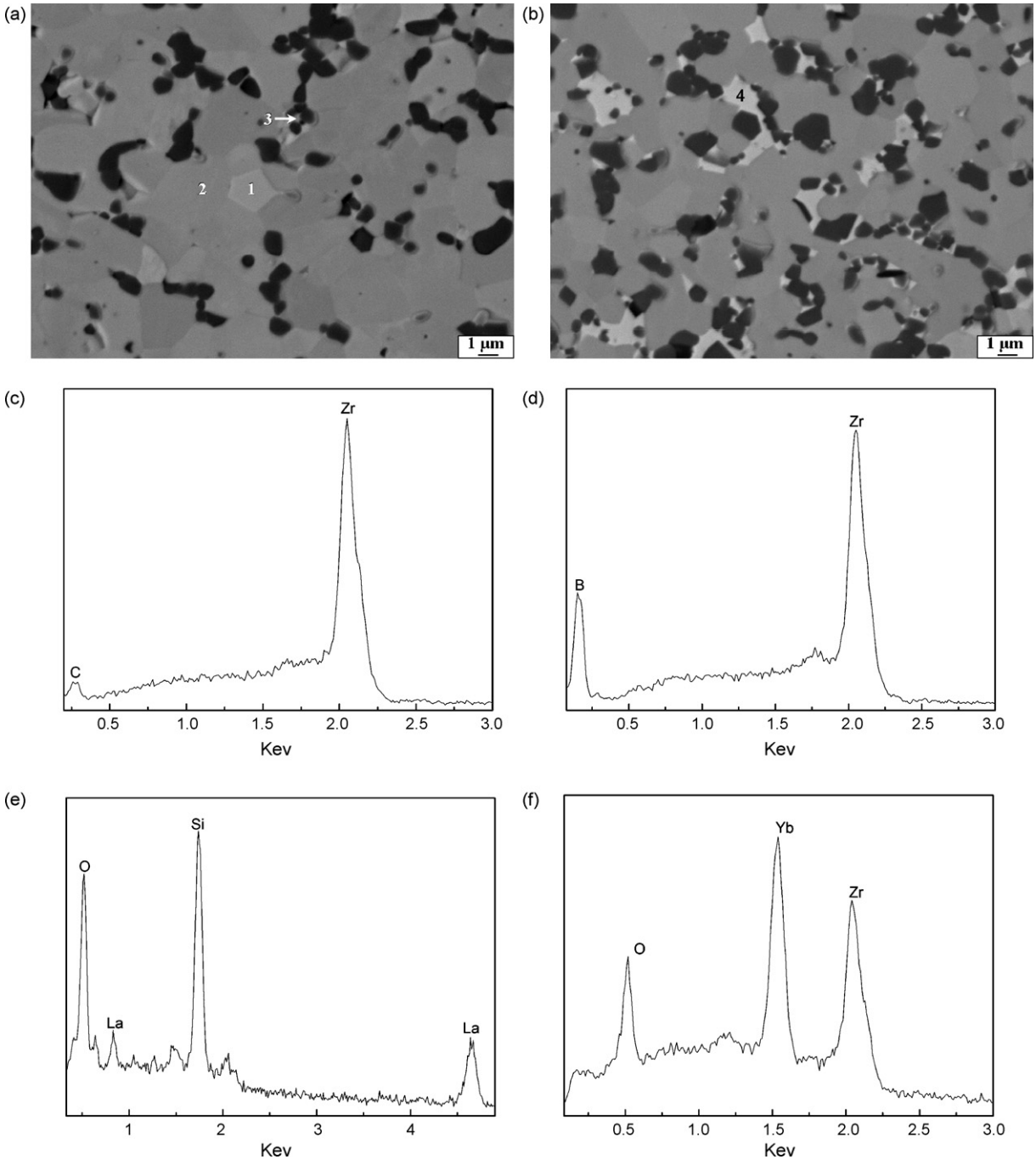

Fig. 2. Backscattered electron micrographs of ZSLa3 (a) and ZSYb3 (b), and corresponding EDS point analyses of the phases marked by 1 (c), 2 (d), 3 (e) and 4 (f).

Fig. 2. A grey ZrB_2 matrix with black dispersed SiC grains can be easily differentiated in ZSLa3 and ZSYb3. Based on XRD and EDS analysis, the additional brighter phase in ZSLa3 can be identified as ZrC (Fig. 2(c)). The SiC particles are encapsulated with a thin film, as indicated by the arrow in Fig. 2(a). EDS analysis revealed that the thin film contains O, Si and La, as shown in Fig. 2(e). Earlier work on liquid phase sintered SiC ceramics showed that La_2O_3 reacts with surface SiO_2 on SiC to form a La_2O_3–SiO_2 phase.[12] Similarly, the La_2O_3 addition might react with SiO_2 to form an amorphous O–Si–La phase on the surface of the SiC grains in ZSLa3, as supported by XRD and EDS analysis.

Based on XRD and EDS analysis (see Fig. 2(f)), the white phase in ZSYb3 could be identified as $Yb_2Zr_2O_7$. BSE observation showed that the distribution of $Yb_2Zr_2O_7$ is comparable to that of SiC. Moreover, the $Yb_2Zr_2O_7$ and SiC phases were always in direct contact (Fig. 2(b)). The SEM micrographs of the acid etched polished surfaces of ZS-1900, ZS-1950, ZSLa3, ZSNd3, ZSY3 and ZSYb3 are presented in Fig. 3. The measured ZrB_2 grain size is given in Table 2. The SiC grain size could not be measured automatically due to agglomeration. The ZrB_2 grains are coarser in the ZS-1950, ZSLa3 and ZSNd3 ceramics compared to ZS-1900, ZSY3 and ZSYb3. Based on SEM observations, a similar trend was observed for the SiC grains.

Based on the phase composition and microstructure, a mechanism by which the addition of Re_2O_3 (Re = La, Nd, Y and Yb) improved densification of ZrB_2–SiC ceramics can be proposed. It is well-known that a SiO_2 film is present on the surface of SiC powder, and ZrO_2 and B_2O_3 oxide impurities are present on the surface of ZrB_2 powder. Previous studies concluded that these

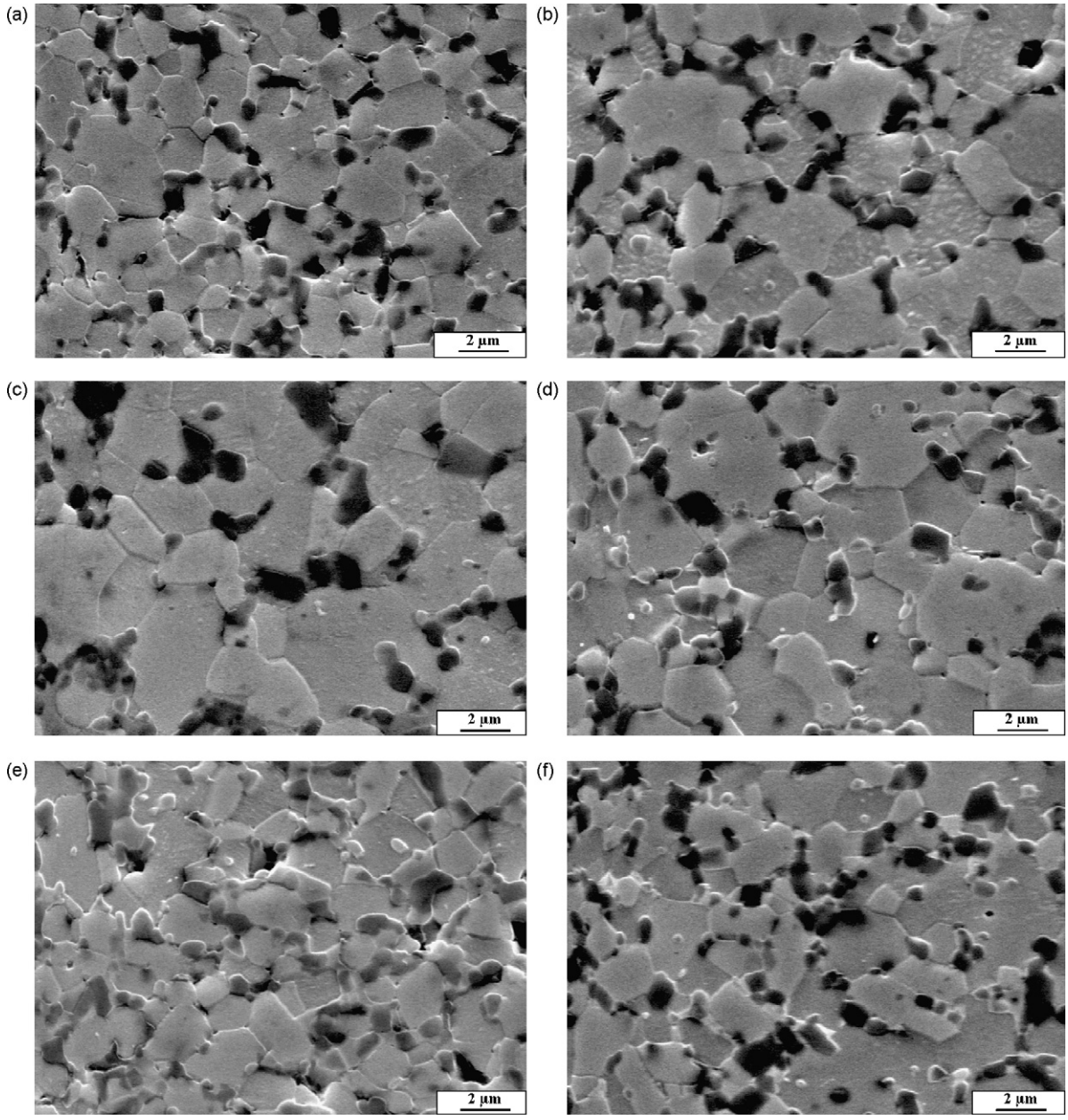

Fig. 3. Secondary electron micrographs of acid etched polished surfaces of ZS-1900 (a), ZS-1950 (b), ZSLa3 (c), ZSNd3 (d), ZSY3 (e) and ZSYb3 (f).

Table 2
Measured ZrB_2 grain sizes in the different ZrB_2–SiC ceramics.

Grade	ZS-1900	ZS-1950	ZSLa3	ZSNd3	ZSY3	ZSYb3
Average ZrB_2 grain size (μm)	1.86 ± 0.42	2.29 ± 0.73	2.60 ± 0.63	2.65 ± 0.75	1.87 ± 0.35	1.88 ± 0.43

surface oxides (SiO_2, ZrO_2 and B_2O_3) inhibit densification.[16–18] In the present study, XRD, EDS and SEM results indicated that La_2O_3 and Nd_2O_3 react with surface oxides to form a liquid phase and promote densification of ZrB_2–SiC ceramics through liquid-phase sintering, accompanied by substantial SiC and ZrB_2 grain growth (see Fig. 3). Enhanced densification of ZrB_2, SiC and ZrB_2–SiC by the introduction of liquid phase was documented in literature.[8,11,12,19] As a result of the presence of liquid or viscous phase, the addition of Si_3N_4 significantly improved densification of ZrB_2.[19]

The mechanism in the Yb_2O_3 and Y_2O_3 doped composites however was different. The XRD, EDS and SEM results revealed that the Yb_2O_3 and Y_2O_3 transfer the ZrO_2 on the surface of the ZrB_2 particles to the grain pockets by forming $Re_2Zr_2O_7$, improving the densification of ZrB_2–SiC ceramics. Although the formation of a minor amount of liquid phase cannot be excluded, the amount will be substantially lower than in the La_2O_3 and Nd_2O_3 doped grades due to the ZrO_2 consumption by the formation of $Re_2Zr_2O_7$, avoiding substantial ZrB_2 grain growth (see Fig. 3). The above analysis indicated that the mechanism of densification improvement for Re_2O_3 with larger cation radius (La_2O_3 and Nd_2O_3) was different than for Re_2O_3 with smaller cationic radius (Y_2O_3 and Yb_2O_3).

3.2. Mechanical properties

The Vickers hardness and fracture toughness of the ceramics are summarized in Table 1. All investigated Re_2O_3 additions increased the Vickers hardness of ZrB_2–SiC from 18.1 GPa up to 19.2–20.2 GPa (see Table 1), especially the Y_2O_3 and Yb_2O_3 additions, which had smaller cation radii. In addition to the phase composition, the Vickers hardness was influenced by the grain size and relative density. As a result, the materials with hard phases, fine-grained microstructure and full density will have a higher hardness. In spite of the coarse-grained microstructure, the ZSLa3 and ZSNd3 ceramics showed a higher hardness than the undoped ZrB_2–SiC composite that might be attributed to the following reasons. Firstly, the addition of La_2O_3 and Nd_2O_3 eliminated the residual porosity and improved densification of ZrB_2–SiC. Secondly, the higher hardness ZrC (25–26 GPa) replaced the lower hardness ZrO_2 (10–12 GPa). For the ZSY3 and ZSYb3 ceramics, the addition of Y_2O_3 and Yb_2O_3 not only improved densification, but also inhibited ZrB_2 grain growth resulting in an increased hardness up to 20.2 GPa (see Table 1).

The fracture toughness of ZrB_2–SiC ceramics was also dependent on the type of Re_2O_3 addition. The addition of the larger cation La_2O_3 and Nd_2O_3 rare-earths resulted in a similar toughness as for the reference undoped ZrB_2–SiC composite, i.e. 3.6 ± 0.1 MPa $m^{1/2}$, whereas the addition of 3 vol% Yb_2O_3 or Y_2O_3 with smaller cation radius induced a significant toughness increase up to 4.7 ± 0.1 MPa $m^{1/2}$ and 4.9 ± 0.2 MPa $m^{1/2}$, respectively. To elucidate the toughening mechanisms, the propagation path of Vickers indentation induced cracks in the ZSLa3, ZSY3 and ZSYb3 ceramics were observed by SEM, as shown in Fig. 4. The indentation crack path in the ZSY3 and ZSYb3 grade appeared more tortuous than in the ZSLa3 ceramic. Inspection of crack propagation revealed crack deflection and perhaps crack bridging by the SiC particles in ZSY3 and ZSYb3, as indicated by the arrows in Fig. 4(b and c). These toughening mechanisms

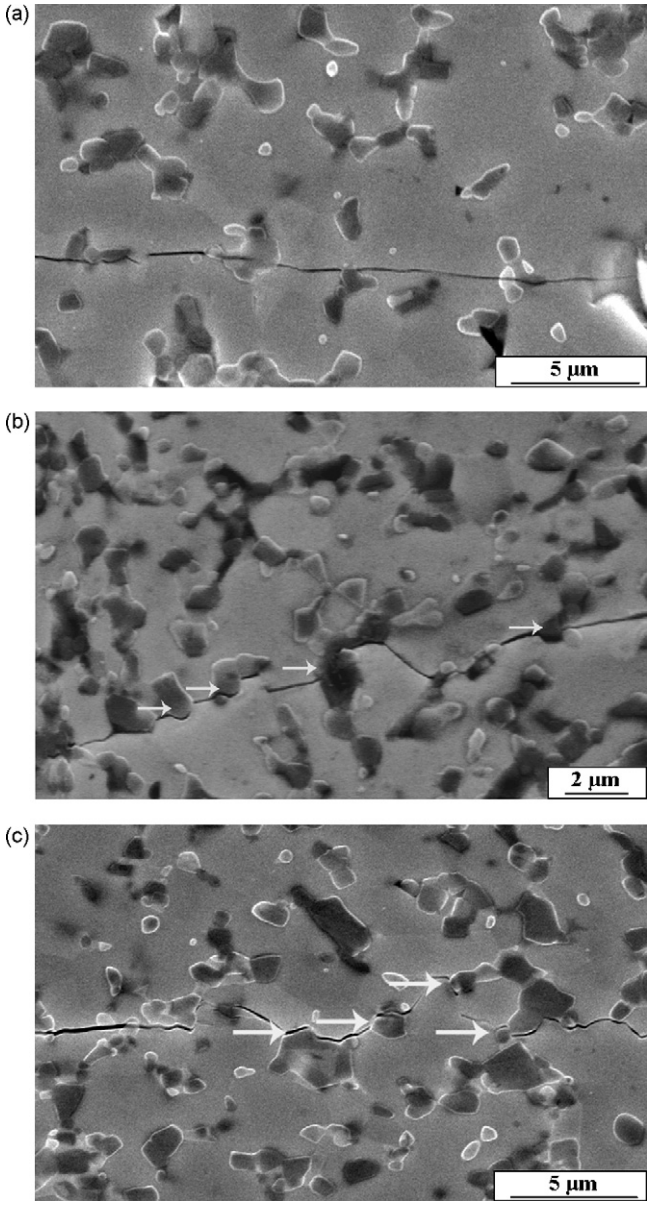

Fig. 4. SEM micrographs of the indentation crack propagation in ZSLa3 (a), ZSY3 (b) and ZSYb3 (c).

increased energy dissipation during crack propagation, resulting in higher fracture toughness. The nature of SiC grain fracture was intergranular for the Yb_2O_3 and Y_2O_3 doped ceramics and transgranular for the Nd_2O_3 and La_2O_3 doped grades. For SiC ceramics, Kueck et al. pointed out that the addition of rare-earth oxides increases the E-modulus of the grain boundary phase.[20] As a result, the elastic mismatch between SiC and the boundary phase would be progressively decreased, reducing the likelihood of crack deflection.[20] In ZSLa3 and ZSNd3, EDS and XRD results indicate that the La_2O_3 and Nd_2O_3 may be enriching the grain boundary phase, especially around the SiC grains (see Fig. 2(a and e)). In ZSY3 and ZSYb3 in contrast, Yb_2O_3 and Y_2O_3 react with surface ZrO_2 of the ZrB_2 particles to form crystalline $Re_2Zr_2O_7$. Applying the findings of Kueck et al. to the ZrB_2–SiC ceramics may explain the different inter- and transgranular fracture behaviour of, respectively, ZSY3 and ZSYb3, and ZSLa3 and ZSNd3. It should be clear that the type of Re_2O_3 strongly influences the nature of the grain boundary and the concomitant fracture and toughening mechanisms.

4. Conclusion

ZrB_2–20 vol% SiC composites with 3 vol% Re_2O_3 (Re = La, Nd, Y or Yb) additions were hot pressed to near full-density at 1900 °C. The addition of the rare-earth oxides enhanced densification of the ZrB_2–SiC composites. The microstructure of the La_2O_3 and Nd_2O_3 doped ZrB_2–SiC composites contained coarse ZrB_2, SiC and ZrC grains as well as an amorphous La/Nd-containing phase locating on the SiC grain boundaries, whereas the Y_2O_3 and Yb_2O_3 doped composites, on the other hand, contained fine ZrB_2 and SiC grains as well as $Re_2Zr_2O_7$ located in direct contact with SiC. Although the hardness could be improved due to a better densification, the fracture toughness of the La_2O_3 and Nd_2O_3 doped ZrB_2–SiC composites was similar or even lower than for the undoped composite due to the transgranular fracture behaviour. Y_2O_3 and Yb_2O_3 addition, on the other hand, enhanced densification without ZrB_2 grain growth and showed an intergranular fracture mechanism resulting in a substantially increased hardness as well as fracture toughness.

Acknowledgements

This work was financially supported by the research fund of K.U. Leuven in the framework of the Flanders-China bilateral project BIL 07/06. Financial support from the Chinese Academy of Sciences under the Program for Recruiting Outstanding Overseas Chinese (Hundred Talents Program), the National Natural Science Foundation of China (No. 50632070), and International Science and Technology Cooperation Project of Shanghai (No. 08520707800) were greatly appreciated.

References

1. Fahrenholtz, W. G. and Hilmas, G. E., Refractory diborides of zirconium and hafnium. *J. Am. Ceram. Soc.*, 2007, **90**, 1347–1364.
2. Chamberlain, A. L., Fahrenholtz, W. G. and Hilmas, G. E., High-strength zirconium diboride-based ceramics. *J. Am. Ceram. Soc.*, 2004, **87**, 1170–1172.
3. Fahrenholtz, W. G., Hilmas, G. E., Chamberlain, A. L. and Zimmermann, J. W., Processing and characterization of ZrB_2-based ultra-high temperature monolithic and fibrous monolithic ceramics. *J. Mater. Sci.*, 2004, **39**, 5951–5957.
4. Monteverde, F., Beneficial effects of an ultra-fine α-SiC incorporation on the sinterability and mechanical properties of ZrB_2. *Appl. Phys. A*, 2006, **82**, 329–337.
5. Monteverde, F. and Bellosi, A., Oxidation of ZrB_2-based ceramics in dry air. *J. Electrochem. Soc.*, 2003, **150**, B552–559.
6. Rezaie, A., Fahrenholtz, W. G. and Hilmas, G. E., Evolution of structure during the oxidation of zirconium diboride–silicon carbide in air up to 1500 °C. *J. Eur. Ceram. Soc.*, 2007, **27**, 2495–2501.
7. Zhu, S. M., Fahrenholtz, W. G. and Hilmas, G. E., Influence of silicon carbide particle size on the microstructure and mechanical properties of zirconium diboride–silicon carbide ceramics. *J. Eur. Ceram. Soc.*, 2007, **27**, 2077–2083.
8. Monteverde, F., Guicciardi, S. and Bellosi, A., Advances in microstructure and mechanical properties of zirconium diboride based ceramics. *Mater. Sci. Eng. A*, 2003, **346**, 310–319.
9. Monteverde, F. and Bellosi, A., Development and characterization of metal-diboride-based composites toughened with ultra-fine SiC particulates. *Solid State Sci.*, 2005, **7**, 622–630.
10. Zhang, X. H., Li, X. Y., Han, J. C., Han, W. B. and Hong, C. Q., Effects of Y_2O_3 on microstructure and mechanical properties of ZrB_2–SiC ceramics. *J. Alloys Compd.*, 2008, **465**, 506–511.
11. Zhou, Y., Hirao, K., Toriyama, M., Yamauchi, Y. and Kanzaki, S., Effects of intergranular phase chemistry on the microstructure and mechanical properties of silicon carbide ceramics densified with rare-earth oxide and alumina additions. *J. Am. Ceram. Soc.*, 2001, **84**, 1642–1644.
12. Tabata, S., Hirata, Y., Sameshima, S., Matsunaga, N. and Ijichi, K., Liquid phase sintering and mechanical properties of SiC with rare-earth oxide. *J. Ceram. Soc. Jpn.*, 2006, **114**, 247–252.
13. Evans, A. G. and Charles, E. A., Fracture toughness determinations by indentation. *J. Am. Ceram. Soc.*, 1976, **59**, 371–372.
14. Tian, W. B., Kan, Y. M., Zhang, G. J. and Wang, P. L., Effect of carbon nanotubes on the properties of ZrB_2–SiC ceramics. *Mater. Sci. Eng. A*, 2008, **487**, 568–573.
15. Xu, Q., Pan, W., Wang, J. D., Wan, C. L., Qi, L. H. and Miao, H. Z., Rare-earth zirconate ceramics with fluorite structure for thermal barrier coatings. *J. Am. Ceram. Soc.*, 2006, **89**, 340–342.
16. Baik, S. and Becher, P. F., Effect of oxygen contamination on densification of TiB_2. *J. Am. Ceram. Soc.*, 1987, **70**, 527–530.
17. Zhu, S. M., Fahrenholtz, W. G., Hilmas, G. E. and Zhang, S. C., Pressureless sintering of zirconium diboride using boron carbide and carbon additions. *J. Am. Ceram. Soc.*, 2007, **90**, 3660–3663.
18. Zhang, S. C., Hilmas, G. E. and Fahrenholtz, W. G., Pressureless Sintering of ZrB_2–SiC Ceramics. *J. Am. Ceram. Soc.*, 2008, **91**, 26–32.
19. Monteverde, F. and Bellosi, A., Effect of the addition of silicon nitride on sintering behaviour and microstructure of zirconium diboride. *Scripta Mater.*, 2002, **46**, 223–228.
20. Kueck, A. M., Kim, D. K., Ramasse, Q. M., De Jonghe, L. C. and Ritchie, R. O., Atomic-resolution imaging of the nanoscale origin of toughness in rare-earth doped SiC. *Nano Lett.*, 2008, **8**, 2935–2939.